Int. J. Heat Mass Transfer. Vol. 27, No. 1, pp. 85–94, 1984
Printed in Great Britain

0017-9310/84 $3.00 + 0.00

HEAT TRANSFER ON A ROTATIONALLY OSCILLATING CYLINDER IN CROSSFLOW

E. P. CHILDS† and R. E. MAYLE
Rensselaer Polytechnic Institute, Troy, NY 12181, U.S.A.

(*Received* 26 *July* 1982 *and in revised form* 9 *May* 1983)

Abstract—The response of laminar skin friction and surface heat transfer to the rotational oscillation of a circular cylinder is analyzed using the series method of Blasius and Howarth and the perturbation method of Lighthill. While the unsteady skin friction component is as much as 38% of the total and increases with frequency, the unsteady heat transfer is found to contribute only 4% near the separation point and decreases with frequency.

NOMENCLATURE

- A amplitude factor, b/U_∞
- b maximum surface speed of cylinder
- C_f skin friction coefficient, $\tau_w/(\rho U_\infty^2/2)$
- D diameter of cylinder
- h convection conductance
- k thermal conductivity
- Nu Nusselt number, hD/k
- p fluid pressure
- Pr Prandtl number, ν/α
- $\dot{q}_0''$ wall heat flux
- R radius of cylinder
- Re_D Reynolds number, $U_\infty D/\nu$
- S Strouhal number, $\omega D/U_\infty$
- t time
- t^* ωt
- T fluid temperature
- T_w cylinder wall temperature
- T_∞ free-stream temperature
- T^* $(T - T_w)/(T_\infty - T_w)$
- T_0^* steady temperature component [see equation (19)]
- T_1^* unsteady temperature component [see equation (19)]
- T_s^* quasi-steady temperature component [see equation (26a)]
- T_2^* acceleration-dependent temperature component [see equation (30)]
- u fluid velocity in x-direction
- $U(x)$ free-stream velocity outside boundary layer
- U_∞ constant reference value of free-stream velocity
- u_1, u_3, etc. dimensionless pressure distribution coefficients
- u^* u/U_∞
- u_0^*, v_0^* steady velocity components [see equations (3)]
- u_1^*, v_1^* unsteady velocity components [see equations (3)]
- u_s^*, v_s^* quasi-steady velocity components [see equations (6a)]
- u_2^*, v_2^* acceleration-dependent velocity components [see equations (10a)]
- v fluid velocity in y-direction
- v^* $(v/U_\infty)\sqrt{(Re_D u_1/2)}$
- x coordinate direction along cylinder surface
- x^* x/R
- y coordinate direction normal to cylinder surface.

Greek symbols

- α thermal diffusivity
- β $S/2u_1$
- η $(y/R)\sqrt{(Re_D u_1/2)}$
- λ_q phase angle of unsteady heat flux
- μ dynamic viscosity
- ν kinematic viscosity
- ρ fluid density
- τ_w wall shear stress, $\mu(\partial u/\partial y)|_{y=0}$
- ω frequency of oscillation.

INTRODUCTION

THE STUDY of unsteady effects in fluid motion has many areas of practical application, particularly in the improvement of the design of turbo-machinery. The oldest class of unsteady laminar boundary layer problem is that in which no mean flow occurs. Stokes's 1st and 2nd Problems [1], Schlichting's analysis of a circular cylinder oscillating in a still fluid [2], and Blasius's study of a circular cylinder set suddenly in motion [3] are typical.

Only in the past 25 years have unsteady problems with a mean flow been considered. Lighthill [4] was the first to formulate a general theory of the response of laminar boundary layers to fluctuations in magnitude, but not direction, of the external flow about a fixed object. By assuming that the magnitude of the fluctuations was small compared to the mean flow, he obtained linear equations for the unsteady components of velocity and temperature. These components were subdivided into quasi-steady and acceleration-dependent parts, both of which were considered to be independent of the frequency of the fluctuations. This approach has since been extended and applied to a

† Present address: Imperial College, London.

variety of flow geometries and boundary conditions [5–13] (partial list).

An exact solution of the Navier–Stokes equations governing two-dimensional (2-D) incompressible flow was found by Rott [14] and Glauert [15], in the case of stagnation flow directed toward a flat plate which oscillates in its own plane. Their work, in contrast with Lighthill's, deals with a situation in which the external flow is steady, but fluctuations in both the magnitude and direction of the flow in the boundary layer occur due to the motion of the object. The absence of any unsteady velocities normal to the plate surface leads to linear unsteady equations without any assumption having been made about the magnitude of the plate surface speed.

In this paper, the analogous problem in a circular cylindrical geometry is considered. The momentum equation has been solved by Hori [7], but no solution of the energy equation appears to have been published. Furthermore, most published values of the various skin friction coefficient components (steady, quasi-steady, and acceleration-dependent) needed in the computation of the heat transfer were found to be of insufficient accuracy to give meaningful temperature fields. In the course of obtaining improved skin friction values, a more general solution of the quasi-steady momentum equation is presented, followed by the solution of the unsteady energy equation. The coordinate system chosen follows previous work and is fixed in the steady-flow field, but the final results can be easily transformed to a system fixed in the rotating cylinder where measurement instruments are most likely to be attached.

THE PROBLEM DESCRIBED

A circular cylinder, shown in cross-section in Fig. 1, is in reciprocating harmonic motion about its axis (here normal to the page) and immersed in a uniform stream flowing steadily in the direction indicated. The Reynolds number of the flow and the radius of curvature of the cylinder are assumed sufficiently large to justify 2-D Cartesian boundary layer analysis. The fluid properties and wall temperature T_w are assumed constant.

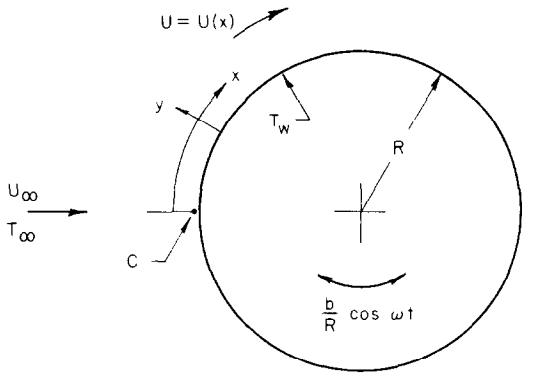

FIG. 1. Flow situation.

A steady reference frame will be used, with a distance x measured from point C in Fig. 1 (the upstream stagnation point in the steady case). The surface velocity of the cylinder relative to this frame is then $b\cos(\omega t)$, and the free-stream velocity outside the boundary layer (unaffected by the cylinder's oscillations) is assumed known in the form

$$U(x) = U_\infty\left[u_1\left(\frac{x}{R}\right)+u_3\left(\frac{x}{R}\right)^3+u_5\left(\frac{x}{R}\right)^5+,\ldots,\right]. \quad (1)$$

Introducing the Blasius dimensionless variables and a dimensionless time variable $t^* = \omega t$ leads to the following unsteady laminar boundary layer equations

$$\frac{\partial u^*}{\partial x^*}+\frac{\partial v^*}{\partial \eta}=0,$$
$$\frac{S}{2}\frac{\partial u^*}{\partial t^*}+u^*\frac{\partial u^*}{\partial x^*}+v^*\frac{\partial u^*}{\partial \eta}=U^*\frac{\mathrm{d}U^*}{\mathrm{d}x^*}+u_1\frac{\partial^2 u^*}{\partial \eta^2}, \quad (2a)$$

with the boundary conditions

$$u^* = A\cos t^*,\quad v^* = 0 \text{ at } \eta = 0,$$
$$u^* \to U^*(x^*) \text{ as } \eta \to \infty. \quad (2b)$$

The energy equation becomes

$$\frac{S}{2}\frac{\partial T^*}{\partial t^*}+u^*\frac{\partial T^*}{\partial x^*}+v^*\frac{\partial T^*}{\partial \eta}=\frac{u_1}{Pr}\frac{\partial^2 T^*}{\partial \eta^2}, \quad (2c)$$

with the boundary conditions

$$T^* = 0 \text{ at } \eta = 0,\quad T^* \to 1 \text{ as } \eta \to \infty. \quad (2d)$$

The three independent parameters which govern the problem are the amplitude factor A, the Strouhal number S and the Prandtl number Pr. In this analysis, A will be assumed small enough for A^2 to be neglected with respect to unity. The unsteady contribution to the velocity and temperature fields will then be a linear perturbation of the steady fields. Secondary streaming effects in the mean flow as well as unsteady velocity components at harmonics of the fundamental frequency are thus ruled out of the final solution, i.e. the time-average of the fluctuating components of velocity and temperature vanish.

Two limiting values of the Strouhal number will be examined. As S approaches zero (quasi-steady case), the problem becomes that of a circular cylinder rotating at a constant rate. This solution will be extended by adding a term which includes the effect of local acceleration, resulting in an unsteady solution valid for S small but finite.

As S approaches very large values, local acceleration dominates near the wall, and interaction with the convective acceleration terms in the mean flow may be neglected. The solution then is seen to consist in the superposition of Stokes's 2nd Problem solution (oscillating flat plate in a fluid at rest at infinity) and that for steady flow around a circular cylinder. The unsteady component of heat transfer will accordingly be vanishingly small since in Stokes's 2nd Problem the

heat transfer occurs entirely and steadily by conduction.

Finally, it will be assumed that the fluid is air or some gas with similar properties, and hence Pr will have a value close to unity.

MOMENTUM EQUATION SOLUTION

The overall solution strategy is to subject equations (2a) to the linear perturbation analysis used by Lighthill [4], expand the resultant zero- and first-order equations following Blasius [3] in a series in x^* whose coefficients are functions of η, and, finally, to solve numerically the resultant ordinary differential equations (two-point boundary-value problems). Relevant details of the latter may be found in the Appendix.

Zero- and first-order equations

The form of u^* and v^* is assumed to be

$$u^*(x^*,\eta,t^*) = u_0^*(x^*,\eta) + Au_1^*(x^*,\eta)\,e^{it^*},$$
$$v^*(x^*,\eta,t^*) = v_0^*(x^*,\eta) + Av_1^*(x^*,\eta)\,e^{it^*}. \tag{3}$$

Substitution of equations (3) in equations (2a) followed by retention of terms of $O(1)$ and of $O(A)$ results in a set of zero-order equations (steady)

$$\frac{\partial u_0^*}{\partial x^*} + \frac{\partial v_0^*}{\partial \eta} = 0,$$
$$u_0^*\frac{\partial u_0^*}{\partial x^*} + v_0^*\frac{\partial u_0^*}{\partial \eta} = U^*\frac{dU^*}{dx^*} + u_1\frac{\partial^2 u_0^*}{\partial \eta^2}, \tag{4a}$$

with boundary conditions

$$u_0^* = v_0^* = 0 \text{ at } \eta = 0, \quad u_0^* \to U^*(x^*) \text{ as } \eta \to \infty, \tag{4b}$$

and first-order equations (unsteady)

$$\frac{\partial u_1^*}{\partial x^*} + \frac{\partial v_1^*}{\partial \eta} = 0,$$
$$\frac{iS}{2}u_1^* + u_0^*\frac{\partial u_1^*}{\partial x^*} + u_1^*\frac{\partial u_0^*}{\partial x^*} + v_0^*\frac{\partial u_1^*}{\partial \eta} + v_1^*\frac{\partial u_0^*}{\partial \eta} = u_1\frac{\partial^2 u_1^*}{\partial \eta^2}, \tag{5a}$$

and boundary conditions

$$u_1^* = 1, \quad v_1^* = 0 \text{ at } \eta = 0, \quad u_1^* \to 0 \text{ as } \eta \to \infty. \tag{5b}$$

The solution of equations (4a) (steady flow over a stationary cylinder) was obtained by Blasius [3], and his calculations were improved and extended by Hiemenz [16], Howarth [17], Froessling [18], Ulrich [19], and Tifford [20]. The functional coefficients of the steady series in x^* are usually denoted as f_1, f_3, etc. where the subscript refers to the power of x^* multiplied. The ordinary differential equations which f_1, f_3, etc. satisfy are discussed thoroughly in Schlichting [21]. They are listed in the Appendix for convenience.

Quasi-steady solution

We now consider the behavior of equations (5a) as S approaches zero, denoting the solution obtained in this instance as u_s^* and v_s^*:

$$\frac{\partial u_s^*}{\partial x^*} + \frac{\partial v_s^*}{\partial \eta} = 0,$$
$$u_0^*\frac{\partial u_s^*}{\partial x^*} + u_s^*\frac{\partial u_0^*}{\partial x^*} + v_0^*\frac{\partial u_s^*}{\partial \eta} + v_s^*\frac{\partial u_0^*}{\partial \eta} = u_1\frac{\partial^2 u_s^*}{\partial \eta^2} \tag{6a}$$

with boundary conditions

$$u_s^* = 1, \quad v_s^* = 0 \text{ at } \eta = 0, \quad u_s^* \to 0 \text{ as } \eta \to \infty. \tag{6b}$$

The general solution in this simple case has been obtained by the authors in closed form and can be verified by direct substitution:

$$u_s^*(x^*,\eta) = \left[\left.\frac{\partial u_0^*}{\partial \eta}\right|_{\eta=0}\right]^{-1}\frac{\partial u_0^*}{\partial \eta}, \tag{7}$$

and by continuity

$$v_s^*(x^*,\eta) = -\frac{d}{dx^*}\left[\left.\frac{\partial u_0^*}{\partial \eta}\right|_{\eta=0}\right]^{-1} \times u_0^* - \left[\left.\frac{\partial u_0^*}{\partial \eta}\right|_{\eta=0}\right]^{-1}\frac{\partial u_0^*}{\partial x^*}. \tag{8}$$

Since u_0^* and v_0^* are available to us as power series expansions, expressions for u_s^* and v_s^* may be written down immediately. In particular

$$u_s^* = g'_{0s}(\eta) + 3\frac{u_3}{u_1}g'_{2s}(\eta)x^{*2} + \ldots, \tag{9a}$$

where

$$g'_{0s} = \frac{f_1''}{f_1''(0)},$$
$$g'_{2s} = \frac{4}{3}\left(\frac{f_3''}{f_1''(0)} - \frac{f_3''(0)f_1''}{[f_1''(0)]^2}\right). \tag{9b}$$

The equation for g'_{0s} and g'_{2s} are equivalent to those found by Rott [14] and Hori [7], respectively.

The physical interpretation of the solution is straightforward. The quasi-steady component of velocity u_s^* (which would result from a clockwise rotation of the cylinder at a constant surface speed AU_∞) is seen by equation (7) to be everywhere proportional to the shear stress distribution in the steady flow. The motion of the cylinder is communicated throughout the boundary layer by viscosity along the developed steady velocity gradients [the pressure term is absent in equations 6(a)]. The quasi-steady skin friction distribution on the upstream surface of the cylinder is compared with the steady values in Fig. 2. The plot was obtained using Hiemenz' [16] experimentally determined pressure coefficients obtained at $Re_D = 1.9 \times 10^4$, which are listed in the Appendix. The effect of the cylinder motion is most pronounced near the stagnation point while the separation points remain nearly in the same position.

Unsteady, low frequency solution

The unsteady velocities u_1^* and v_1^* are now assumed to be composed of quasi-steady components u_s^* and v_s^*,

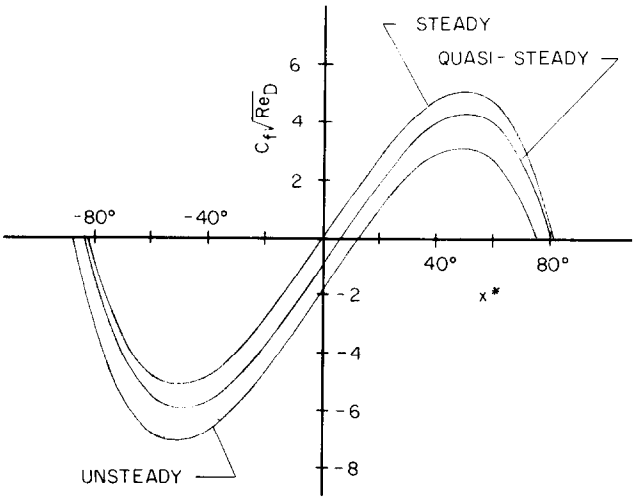

FIG. 2. Unsteady skin friction, Hiemenz pressure distribution, $A = 0.3162$, $\beta = 2.7$.

and acceleration-dependent components u_2^* and v_2^*:

$$u_1^* = u_s^* + i\beta u_2^*, \qquad v_1^* = v_s^* + i\beta v_2^*, \tag{10a}$$

where β is defined by

$$\beta = \frac{S}{2u_1}. \tag{10b}$$

If equations (10a) are substituted in equations (5a), the terms in $(i\beta)^1$ yield the equations for the acceleration-dependent components u_2^* and v_2^*:

$$\frac{\partial u_2^*}{\partial x^*} + \frac{\partial v_2^*}{\partial \eta} = 0,$$

$$u_0^*\frac{\partial u_2^*}{\partial x^*} + u_2^*\frac{\partial u_0^*}{\partial x^*} + v_0^*\frac{\partial u_2^*}{\partial \eta} + v_2^*\frac{\partial u_0^*}{\partial \eta} = u_1\left(\frac{\partial^2 u_2^*}{\partial \eta^2} - u_s^*\right), \tag{11a}$$

with boundary conditions

$$u_2^* = v_2^* = 0 \text{ at } \eta = 0, \quad u_2^* \to 0 \text{ as } \eta \to \infty. \tag{11b}$$

Let

$$u_2^* = g'(\eta) + 3\frac{u_3}{u_1}g'_{22}(\eta)x^{*2}, \qquad v_2^* = -6\frac{u_3}{u_1}g_{22}(\eta)x^*. \tag{12}$$

Substitution of these expressions into equations (11a) yields

$$g'''_{02} + f_1 g''_{02} - f'_1 g'_{02} = g'_{0s}, \tag{13a}$$

with boundary conditions

$$g'_{02}(0) = g'_{02}(\infty) = 0, \tag{13b}$$

and

$$g'''_{22} + f_1 g''_{22} - 3f'_1 g'_{22} + 2f''_1 g_{22} = 4(f'_3 g'_{02} - f_3 g''_{02}) + g'_{2s}, \tag{14a}$$

with boundary conditions

$$g'_{22}(0) = g_{22}(0) = g'_{22}(\infty) = 0. \tag{14b}$$

Equation (13a) was obtained and solved by Glauert [15] and Rott [14] in connection with the oscillating plate stagnation flow problem. Hori [7] obtained equation (14a) and solved it numerically. The numerical solution of equations (13a) and (14a), needed for later calculation of the unsteady heat transfer, requires accurate values of $g''_{02}(0)$ and $g''_{22}(0)$ [as well as $f''_1(0)$ and $f''_3(0)$]. These are listed in the Appendix. The maximum value of β for which equations (10a) hold will now be determined by seeking a solution of equations (5a) valid as β approaches infinity.

Unsteady, high frequency solution

Since the time-dependent boundary layer thickness is much smaller than that of the steady viscous layer when the frequency parameter β is large, the interaction between the two layers embodied in the convection terms of equations (5a) may be neglected, leaving

$$\frac{\partial^2 u_1^*}{\partial \eta^2} - i\beta u_1^* = 0, \tag{15a}$$

with boundary conditions

$$u_1^* = 1, \quad v_1^* = 0 \text{ at } \eta = 0, \quad u_1^* \to 0 \text{ as } \eta \to \infty \tag{15b}$$

which admits a solution which is independent of x^*, namely

$$u_1^* = e^{-\sqrt{(i\beta)}\eta}, \quad v_1^* = 0. \tag{16}$$

The high frequency skin friction becomes

$$C_f\sqrt{Re_D} = C_{f0}\sqrt{Re_D} - 2\sqrt{(2u_1)}A\beta^{1/2}\cos\left(t^* + \frac{\pi}{4}\right). \tag{17}$$

The negative sign on the unsteady component arises due to the fact that clockwise motion of the cylinder

gives rise to a negative wall shear stress. (See Schlichting [21] for the steady skin friction $C_{f0}\sqrt{Re_D}$.) The maxima of skin friction anticipates those of the cylinder's surface velocity of 45°, a result which parallels Lighthill's findings [4].

Matching range

The magnitude of the unsteady component of the high frequency skin friction $\beta^{1/2}$ will now be compared with that of the low frequency solution

$$\sqrt{\left\{\left[\frac{\partial u_s^*}{\partial \eta}\bigg|_{\eta=0}\right]^2+\beta^2\left[\frac{\partial u_2^*}{\partial \eta}\bigg|_{\eta=0}\right]^2\right\}}. \tag{18}$$

Using Hiemenz' [16] experimentally determined pressure distribution coefficients, the plot shown as Fig. 3 results. The two solutions agree quite well in mid-range. Since the high frequency solution is independent of x^*, we expect mid-range matching solutions at $x^* = 0°, 40°$ and 80° to merge into the high frequency parabola. This behavior is suggested by solid line fairings. At all three x^* locations the low and high frequency solutions intersect roughly in the middle of their matching regions. (At $\beta = 3.25, 2.82$ and 2.00 for $x^* = 0°, 40°$ and 80°, respectively, indicated by the perpendiculars in Fig. 3.) It seems reasonable to adopt the average of these three values, $\beta_0 = 2.7$, as an estimate of the maximum value of β for which equation (18) is valid. The total low frequency unsteady skin friction is compared with the steady and quasi-steady solutions in Fig. 2. The contribution of the acceleration-dependent term (at $\beta = \beta_0$) is seen to be of the same order as the quasi-steady term. The two terms together at $x^* = 50°$ (where the steady skin friction is largest) produce a fluctuation which amounts to ±38%.

Energy equation solution

The energy equation may be solved in an analogous manner. We assume that the temperature can be expressed as the sum of a steady and a fluctuating component

$$T^*(x^*, \eta, t^*) = T_0^*(x^*, \eta) + AT_1^*(x^*, \eta)\, e^{it^*}, \tag{19}$$

and that terms of $O(A^2)$ may be neglected. Two equations for T_0^* and T_1^* again result

$$u_0^*\frac{\partial T_0^*}{\partial x^*}+v_0^*\frac{\partial T_0^*}{\partial \eta}=\frac{u_1}{Pr}\frac{\partial^2 T_0}{\partial \eta^2}, \tag{20a}$$

with boundary conditions

$$T_0^* = 0 \text{ at } \eta = 0, \quad T_0^* \to 1 \text{ as } \eta \to \infty, \tag{20b}$$

and

$$\frac{iS}{2}T_1^*+u_0^*\frac{\partial T_1^*}{\partial x^*}+u_1^*\frac{\partial T_0^*}{\partial x^*}+v_0^*\frac{\partial T_1^*}{\partial \eta}+v_1^*\frac{\partial T_0^*}{\partial \eta}=\frac{u_1}{Pr}\frac{\partial^2 T_1^*}{\partial \eta^2}, \tag{21a}$$

with boundary conditions

$$T_1^* = 0 \text{ at } \eta = 0, \quad T_1^* \to 0 \text{ as } \eta \to \infty. \tag{21b}$$

Equation (20a) was solved by Froessling [18] by expanding $T_0^*(x^*, \eta)$ in an even power series in x^* whose coefficients are functions of η. Only the first two terms and differential equations are given here

$$T_0^* = F_0(\eta)+4\frac{u_3}{u_1}F_2(\eta)x^{*2}, \tag{22}$$

$$\frac{1}{Pr}F_0''+f_1F_0' = 0, \tag{23a}$$

with boundary conditions

$$F_0(0) = 0, \quad F_0(\infty) = 1, \tag{23b}$$

and

$$\frac{1}{Pr}F_2''+f_1F_2'-2f_1'F_2 = -3f_3F_0', \tag{24a}$$

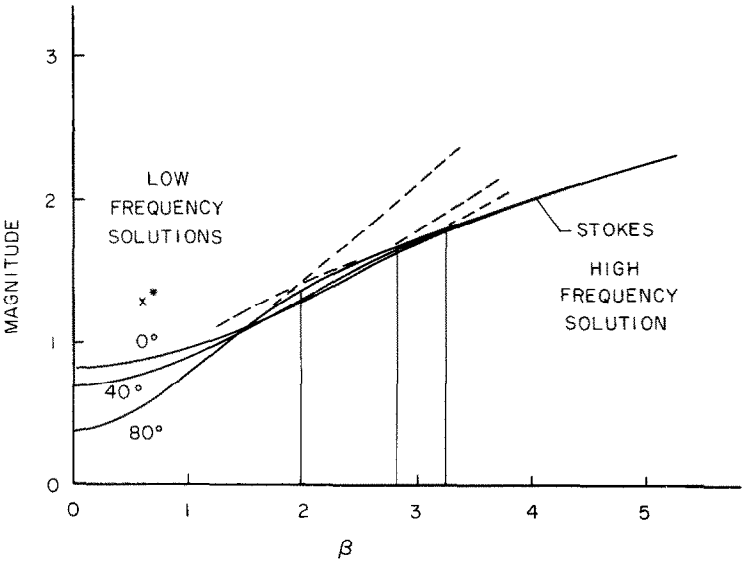

FIG. 3. Magnitude of unsteady skin friction.

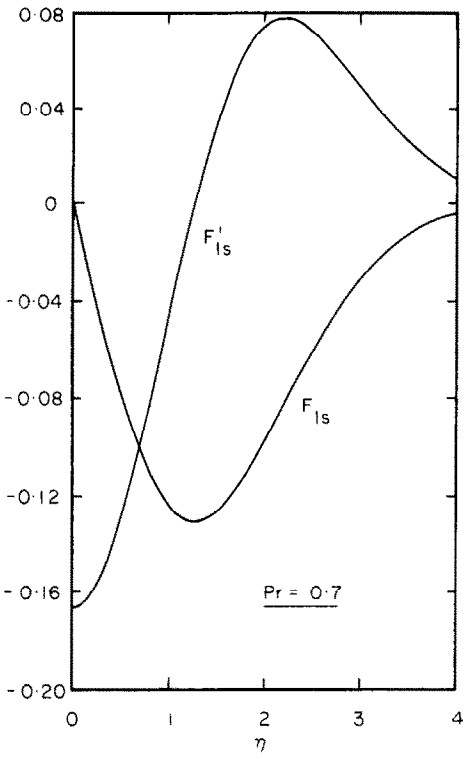

FIG. 4. Quasi-steady temperature function F_{1s}.

with boundary conditions

$$F_2(0) = F_2(\infty) = 0. \tag{24b}$$

In terms of the Nusselt number Nu, the steady solution is

$$\frac{Nu_0}{\sqrt{Re_D}} = \sqrt{(2u_1)}\left(F'_0(0) + 4\frac{u_3}{u_1}F'_2(0)x^{*2} + \ldots,\right), \tag{25}$$

where coefficients $F'_0(0)$ and $F'_2(0)$, recalculated by the authors for $Pr = 0.7$ are given in the Appendix.

Quasi-steady solution

The behavior of equation (21a) is now examined as S tends to zero, and the solution obtained denoted by T_s^*:

$$u_0^*\frac{\partial T_s^*}{\partial x^*} + u_s^*\frac{\partial T_0^*}{\partial x^*} + v_0^*\frac{\partial T_s^*}{\partial \eta} + v_s^*\frac{\partial T_0^*}{\partial \eta} = \frac{u_1}{Pr}\frac{\partial^2 T_s^*}{\partial \eta^2}, \tag{26a}$$

with boundary conditions

$$T_s^* = 0 \text{ at } \eta = 0, \quad T_s^* \to 0 \text{ as } \eta \to \infty. \tag{26b}$$

A series method will be used to obtain the solution as no closed form solution analogous to that obtained in the quasi-steady form of the momentum equation is known. By inspection of equation (26a) an odd series representation is appropriate:

$$T_s^* = 2\frac{u_3}{u_1^2}F_{1s}(\eta)x^* + \ldots, \tag{27}$$

resulting in

$$\frac{1}{Pr}F''_{1s} + f_1F'_{1s} - f'_1F_{1s} = 4g'_{0s}F_2 - 3g_{2s}F'_0, \tag{28a}$$

with boundary conditions

$$F_{1s}(0) = F_{1s}(\infty) = 0. \tag{28b}$$

This equation, solved numerically for $Pr = 0.7$, is plotted in Fig. 4.

The quasi-steady component of Nu becomes

$$\frac{Nu_s}{\sqrt{Re_D}} = \sqrt{(2u_1)}2\frac{u_3}{u_1^2}F''_{1s}(0)x^* + \ldots, \tag{29}$$

which is compared to the steady component in Fig. 5 using Hiemenz' pressure distribution coefficients. Positive (clockwise) rotation of the cylinder is seen to increase Nu on the top half of the cylinder while decreasing it on the bottom. Physically, this result is

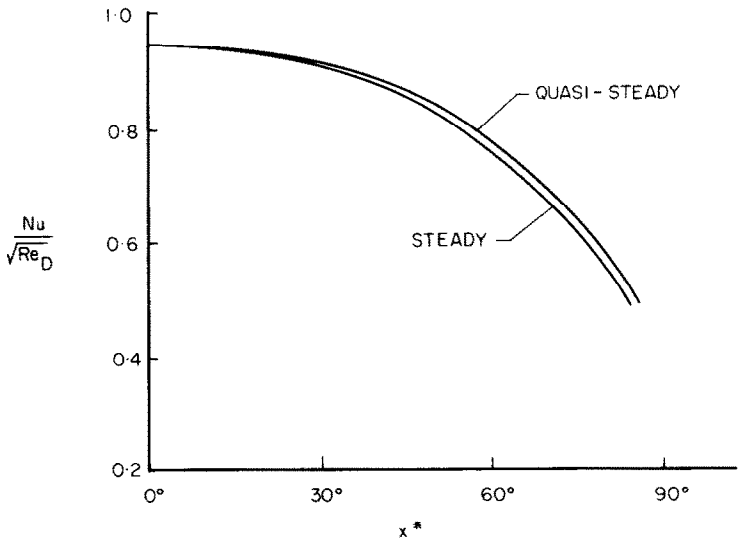

FIG. 5. Quasi-steady surface heat transfer, Hiemenz pressure distribution, $A = 0.3162$, $Pr = 0.7$.

plausible. On the top half of the cylinder ($x^* > 0$), the fluid in the boundary layer is moved along at a higher speed than that of the mean flow—thus the capacity of the fluid to convect heat is increased. On the lower half ($x^* < 0$) the opposite occurs and the heat transfer is accordingly retarded. This effect, though, is very small. For the Hiemenz distribution, deviation of the quasi-steady value from its steady value is at most 4% (near the separation point).

Unsteady, low frequency solution

The quasi-steady solution may be extended, as with the momentum equation, by writing

$$T_1^* = T_s^* + i\beta T_2^*. \tag{30}$$

The equation satisfied by T_2^* is then

$$u_0^* \frac{\partial T_2^*}{\partial x^*} + u_2^* \frac{\partial T_0^*}{\partial x^*} + v_0^* \frac{\partial T_2^*}{\partial \eta} + v_2^* \frac{\partial T_0^*}{\partial \eta} = u_1\left(\frac{1}{Pr}\frac{\partial^2 T_2^*}{\partial \eta^2} - T_s^*\right), \tag{31a}$$

with boundary conditions

$$T_2^* = 0 \text{ at } \eta = 0, \quad T_2^* \to 0 \text{ as } \eta \to \infty. \tag{31b}$$

A series expansion is again made, the first term of which is

$$T_2^* = 2\frac{u_3}{u_1^2} F_{12}(\eta) x^* + \ldots, \tag{32}$$

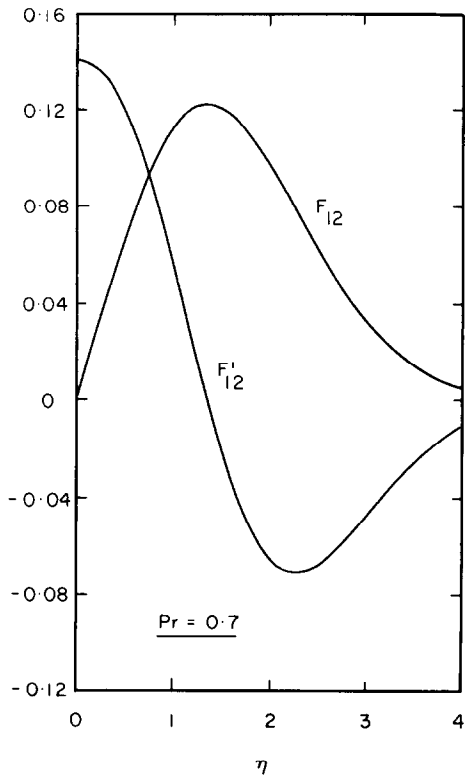

FIG. 6. Acceleration-dependent temperature function F_{12}.

and the ordinary differential equation F_{12} satisfies is

$$\frac{1}{Pr} F_{12}'' + f_1 F_{12}' - f_1' F_{12} = 4g_{02}' F_2 - 3g_{22} F_0' + F_{1s}, \tag{33a}$$

with boundary conditions

$$F_{12}(0) = F_{12}(\infty) = 0. \tag{33b}$$

The solution for $Pr = 0.7$ is given as Fig. 6, and the expression for the unsteady, low frequency Nu follows:

$$\frac{Nu}{\sqrt{Re_D}} = \frac{Nu_0}{\sqrt{Re_D}} + A\sqrt{(2u_1)}\sqrt{\left\{\left(\frac{\partial T_s^*}{\partial \eta}\bigg|_{\eta=0}\right)^2 + \beta^2\left(\frac{\partial T_2^*}{\partial \eta}\bigg|_{\eta=0}\right)^2\right\}}\cos(t^* + \lambda_q), \tag{34}$$

where

$$\lambda_q = \tan^{-1}\frac{\beta\left(\dfrac{\partial T_2^*}{\partial \eta}\bigg|_{\eta=0}\right)}{\left(\dfrac{\partial T_0^*}{\partial \eta}\bigg|_{\eta=0}\right)} = \tan^{-1}(-0.8361\beta).$$

Unsteady, high frequency solution

Again it is appropriate to determine the maximum value of β for which equation (34) is valid, and hence to assess the significance of the acceleration-dependent term (T_2^*). As β approaches large values equation (21a) becomes

$$\frac{u_1}{Pr}\frac{\partial^2 T_1^*}{\partial \eta^2} - \frac{iS}{2} T_1^* = u_1^* \frac{\partial T_0^*}{\partial x^*} + v_1^* \frac{T_0^*}{\partial \eta}, \tag{35a}$$

with boundary conditions

$$T_1^* = 0 \text{ at } \eta = 0, \quad T_1^* \to 0 \text{ as } \eta \to \infty. \tag{35b}$$

Since we wish to determine the unsteady wall heat flux caused by the high frequency oscillations, equation (35a) may be simplified by using an expression for $\partial T_0^*/\partial x^*$ which is valid near the wall, namely

$$\frac{\partial T_0^*}{\partial x^*} \simeq \frac{\partial T_0}{\partial x^*}\bigg|_{\eta=0} + \eta \frac{\partial^2 T_0^*}{\partial \eta \partial x^*}\bigg|_{\eta=0}. \tag{36}$$

Using the expressions for u_1^* and v_1^* determined earlier, equation (35a) becomes

$$\frac{\partial^2 T_1^*}{\partial \eta^2} - i\beta\, Pr\, T_1^* = \frac{Pr}{u_1}\frac{\partial^2 T_0^*}{\partial \eta \partial x^*}\bigg|_{\eta=0} e^{-\sqrt{(i\beta)}\eta}, \tag{37}$$

whose solution is

$$T_1^* = \frac{Pr}{i\beta(1-Pr)}\frac{1}{u_1}\left[\frac{\partial^2 T_0^*}{\partial \eta \partial x^*}\bigg|_{\eta=0}\right]\left[\eta\, e^{-\sqrt{(i\beta)}\eta} + \frac{1}{\sqrt{(i\beta)}}\frac{2}{(1-Pr)}(e^{-\sqrt{(i\beta)}\eta} - e^{-\sqrt{(i\beta\, Pr)}\eta})\right], \tag{38}$$

valid for η small and $Pr \neq 1$. The unsteady component of heat transfer may be determined from

$$\frac{\partial T_1^*}{\partial \eta}\bigg|_{\eta=0} e^{it^*}, \tag{39}$$

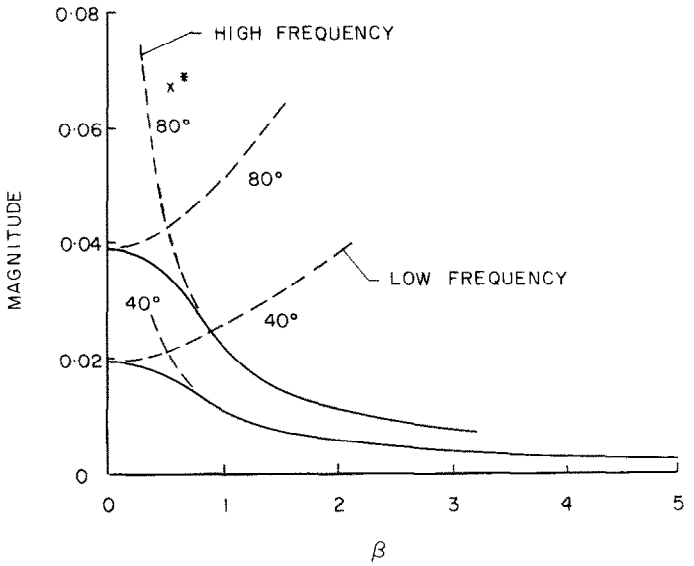

FIG. 7. Magnitude of unsteady heat transfer.

the real part of which is

$$\frac{1}{\beta}\left(\frac{1}{u_1}\left.\frac{\partial^2 T_0}{\partial\eta\partial x^*}\right|_{\eta=0}\right) \times\left[\frac{Pr}{(1-Pr)}+\frac{2Pr(\sqrt{Pr}-1)}{(1-Pr)^2}\right]\cos\left(t^*-\frac{\pi}{2}\right). \quad (40)$$

For $Pr = 0.7$, the value in square brackets is -0.2075. As the value of the first term in parentheses is also negative, we find that, unlike the skin friction, the heat transfer maxima at the wall lag behind those of the cylinder surface velocity by 90°. Moreover, the magnitude of the unsteady component falls off as $1/\beta$, in marked contrast with the skin friction. These results parallel those found by Lighthill [4].

Matching range

When equation (40) is compared in magnitude with the corresponding term in the low frequency expression [the large radical in equation (34)], the plot given as Fig. 7 results. Both magnitudes have been plotted as a function of β at $x^* = 40°$ and 80° (at $x^* = 0°$ the unsteady component vanishes). At both locations, the high and low frequency curves intersect at low (about 0.5) values of β at which point the magnitude of the low frequency component differs little from its quasi-steady value. Such a result suggests that the magnitude of the unsteady heat transfer never rises above its quasi-steady value but rather decreases with β, gradually attaining the high frequency value. This proposed behavior is reflected in the solid line fairings.

We are thus left with the interesting conclusion that the quasi-steady magnitude is the maximum value attained over the entire range of β. But the quasi-steady solution has already been seen to differ from the steady solution, by at most 4%, and therefore may be neglected. The steady expressions for the heat transfer ($Nu_0/\sqrt{Re_D}$) are thus adequate even when the cylinder is oscillating, regardless of the frequency, as long as the amplitude factor A is small.

CONCLUDING REMARKS

The negligible effect of cylinder oscillation on the surface heat transfer may be seen in retrospect to be a consequence of the constant surface temperature boundary conditions and the boundary layer assumption. From equation (21a), it is evident that the magnitude of the unsteady temperature component T_1^*, because of the homogeneous boundary conditions, will depend heavily on the two inhomogeneous terms $v_1^*(\partial T_0^*/\partial x^*)$ and $v_1^*(\partial T_0^*/\partial\eta)$. The former will be small since T_w is constant, the latter will be small also due to the boundary layer scaling approximation which assumes that velocity components across the layer are of $O(Re^{-1/2})$.

The fact that the quasi-steady magnitude of Nu, small as it is, is the maximum, is consistent with the well-known result that the thickness of the 'AC' boundary layer varies inversely with the square root of the oscillation frequency. As the latter increases, and the 'AC' layer becomes smaller relative to the cylinder's radius, Stokes's 2nd Problem result is approached where any unsteady heat transfer is known to be absent.

Acknowledgement—This work was funded by NASA Lewis Research Center, Heat Transfer Fundamental Section under grant No. NSG-3262.

REFERENCES

1. H. Schlichting, *Boundary Layer Theory* (7th edn.), p. 90. McGraw-Hill, New York (1979).
2. H. Schlichting, *Boundary Layer Theory* (7th edn.), p. 428. McGraw-Hill, New York (1979).
3. H. Blasius, The boundary layers in fluids with little friction, NACA TM 1256.

4. M. J. Lighthill, The response of laminar skin friction and heat transfer to fluctuations in the stream velocity, *Proc. R. Soc.* **A224**, 1–23 (1954).
5. E. Hori, Unsteady boundary layers, 1st report, theory of the boundary layer on a symmetrical body in a fluctuating main stream, *Bull. J.S.M.E.* **4**, 664–671 (1961).
6. E. Hori, Unsteady boundary layers, 2nd report, flow around a body with fluctuating circulation, *Bull. J.S.M.E.* **5**, 57–63 (1962).
7. E. Hori, Unsteady boundary layers, 3rd report, boundary layer on a circular cylinder in rotational oscillation, *Bull. J.S.M.E.* **5**, 64–71 (1962).
8. E. Hori, Unsteady boundary layers, 4th report, calculation of boundary layer around a body with arbitrary shape by use of a series expansion method, *Bull. J.S.M.E.* **5**, 461–470 (1962).
9. J. T. Stuart, A solution of the Navier–Stokes and energy equations illustrating the response of skin friction and temperature of an infinite plate thermometer to fluctuations in the stream velocity, *Proc. R. Soc.* **A231**, 116–130 (1955).
10. N. Rott and M. L. Rosenzweig, On the response of the laminar boundary layer to small fluctuations of the free-stream velocity, *J. Aero/Space Sci.* **27**, 741–747 (1960).
11. J. Watson, The two-dimensional boundary layer flow near the stagnation point of a cylinder which has an arbitrary transverse motion, *Q. Jl Mech. Appl. Math.* **12**, 175–190 (1959).
12. J. Watson, A solution of the Navier–Stokes equations illustrating the response of a laminar boundary layer to a given change in the external stream velocity, *Q. Jl Mech. Appl. Math.* **11**, 302–325 (1958).
13. Ishigaki, Periodic boundary layer near a two-dimensional stagnation point, *J. Fluid Mech.* **43**, 477–486 (1970).
14. N. Rott, Unsteady viscous flow in the vicinity of a stagnation point, *Q. Appl. Math.* **13**, 444–451 (1955).
15. M. B. Glauert, The laminar boundary layer on oscillating plates and cylinders, *J. Fluid Mech.* **1**, 97–110 (1956).
16. K. Hiemenz, Die Grenzschicht an einem in den gleichförmigen flüssigkeitsstrom ein getauchten geraden Kreiszylinder, Thesis Göttingen, *Dinglers Polytechn. J.* **326**, 32 (1911).
17. L. Howarth, On the calculation of steady flow in tne boundary layer near the surface of a cylinder in a stream, ARC R&M 1632 (1935).
18. N. Froessling, Evaporation, heat transfer and velocity distribution in two-dimensional and rotationally symmetrical laminar boundary-layer flow, NACA TM 1432.
19. A. Ulrich, Die ebene laminare reibungsschicht an einem zylinder, *Arch. Math.* **2**, 33–41 (1949–1950).
20. A. N. Tifford, Heat transfer and frictional effects in laminar boundary layers. Part 4: Universal series solutions, WADC Technical Report, pp. 53–288 (1954).
21. H. Schlichting, *Boundary Layer Theory* (4th edn.), p. 147. McGraw-Hill, New York (1960).
22. IMSL, Inc., *IMSL Library Reference Manual*, Houston (1979).
23. F. M. White, *Viscous Fluid Flow*, p. 177. McGraw-Hill, New York (1974).
24. S. Goldstein, *Modern Developments in Fluid Dynamics*, p. 151. Dover, New York (1965).

APPENDIX

The ordinary differential equations were solved using the IMSL [22] initial value problem package DGEAR on an IBM 370 Model 3033 computer installed at RPI. DGEAR uses a variable order Adams Predictor–Corrector method and requires that all necessary boundary conditions be specified at $\eta = 0$. The program was adapted to the two-point boundary value problems in this paper by guessing an additional initial condition to satisfy the condition at $\eta = \infty$. The asymptotic behavior of all the functions is proportional to the complementary error function erfc $(\eta/\sqrt{2})$, and hence $\eta = 10$ was found to be a satisfactory approximation of ∞. The additional initial values, determined by trial and error (i.e. by a 'shooting' method), and the relevant DGEAR user-set parameters are given in Table A1. Double precision was used and the values listed are believed accurate to eight decimal places. The results compare favorably with most of the published tables (refs. [5, 15, 18, 20, 23]), but are presumed to be more accurate (all to six decimal places).

Table A1

$f''_1(0) =$	1.23258766 [24]	$F'_0(0) =$	0.49586579† ($Pr = 0.7$)
$f''_3(0) =$	0.72444731†	$F'_2(0) =$	0.11190690† ($Pr = 0.7$)
$g''_{02}(0) =$	−0.49323064†	$F'_{1s}(0) =$	−0.16780041† ($Pr = 0.7$)
$g''_{22}(0) =$	0.19676977†	$F'_{12}(0) =$	0.14029574† ($Pr = 0.7$)

The first three terms of the series solution of equations (4a) are

$$u_0^* = u_1 f'_1(\eta)x^* + 4u_3 f'_3(\eta)x^{*3} + 6u_5\left[g'_5(\eta) + \frac{u_3^2}{u_1 u_5}h'_5(\eta)\right]x^{*5}, \tag{A1}$$

and

$$v_0^* = -\left(u_1 f_1(\eta) + 12u_3 f_3(\eta)x^{*2} + 30u_5 \times \left[g_5(\eta) + \frac{u_3^2}{u_1 u_5}h_5(\eta)\right]x^{*4}\right), \tag{A2}$$

where f_1, f_3, g_5 and h_5 satisfy the following ordinary differential equations

$$f'''_1 + f_1 f''_1 - f'^2_1 = -1, \quad f_1(0) = f'_1(0) = 0, \quad f'_1(\infty) = 1 \quad (f''_1(0) = 1.23258766)\ [24], \tag{A3}$$

$$f'''_3 + f_1 f''_3 - 4f'_1 f'_3 + 3f''_1 f_3 = -1, \quad f_3(0) = f'_3(0) = 0, \quad f'_3(\infty) = 1/4 \quad (f''_3(0) = 0.72444731),\dagger \tag{A4}$$

$$g'''_5 + f_1 g''_5 - 6f'_1 g'_5 + 5f''_1 g_5 = -1, \quad g_5(0) = 0, \tag{A5}$$

$$g'_5(0) = 0, \quad g'_5(\infty) = 1/6 \quad (g''_5(0) = 0.6347)\ [20],$$

$$h'''_5 + f_1 h''_5 - 6f'_1 h'_5 + 5f''_1 h_5 = 8(f'^2_3 - f_3 f''_3) - \tfrac{1}{2}, \quad h_5(0) = h'_5(0) = h'_5(\infty) = 0 \quad (h''_5(0) = 0.1192)\ [20]. \tag{A6}$$

The Hiemenz [16] pressure distribution coefficients used for all calculations in this paper are listed in Table A2.

Table A2. Pressure distribution coefficients

Coefficient (group)	Hiemenz
u_1	1.8157
u_3	−0.2714
u_5	−0.0473
$u_3^2/u_1 u_5$	−0.8572

† Determined by the authors. TOL = 10^{-10} [22], METH = 1 [22], MITER = 0 [22].

TRANSFERT THERMIQUE SUR UN CYLINDRE EN ROTATION OSCILLANTE ET EN ATTAQUE FRONTALE

Résumé—La réponse du frottement pariétal laminaire et du transfert thermique à l'oscillation rotationnelle d'un cylindre circulaire est analysée à partir d'une méthode de Blasius et Howard et la méthode de perturbation de Lighthill. Tandis que la composante du frottement pariétal instationnaire est à peu près 38% du total et qu'elle croît avec la fréquence, le transfert thermique instationnaire contribue seulement pour 4% près du point de séparation et décroît avec la fréquence.

DER WÄRMEÜBERGANG AN EINEM DREHSCHWINGUNGEN AUSFÜHRENDEN ZYLINDER IM KREUZSTROM

Zusammenfassung—Der Einfluß von Drehschwingungen eines Zylinders auf den laminaren Wärmeübergang und Druckabfall wird mit Hilfe der Reihenentwicklung nach Blasius und Howarth und des Störungsansatzes von Lighthill untersucht. Während der Anteil der instationären Komponente beim Druckabfall bis zu 38% des Gesamtwertes ausmacht und mit der Frequenz ansteigt, beträgt der instationäre Anteil des Wärmeüberganges nur 4% am Ablösungspunkt und nimmt mit der Frequenz ab.

ТЕПЛООБМЕН ПОПЕРЕЧНО ОБТЕКАЕМОГО ВРАЩАТЕЛЬНО КОЛЕБЛЮЩЕГОСЯ ЦИЛИНДРА

Аннотация—Методом разложения в ряды Блазиуса и Ховарта и методом возмущений Лайтхилла проанализировано влияние вращательного колебания круглого цилиндра на ламинарное поверхностное трение и теплоперенос на поверхности. Найдено, что в нестационарном режиме вклад поверхностного трения составляет 38% от суммарного значения и растет с частотой, тогда как вклад теплопереноса составляет только 4% у точки отрыва и падает с частотой.